



# Variability of Middle East springtime dust events between 2011 and 2022

Parya Broomandi<sup>1,2</sup> · David Galán-Madruga<sup>3</sup> · Alfredo Satyanaga<sup>1</sup> · Mehdi Hamidi<sup>4</sup> · Dorna Gholamzade Ledari<sup>5</sup> · Aram Fathian<sup>6,7,8</sup> · Rasoul Sarvestan<sup>9</sup> · Nasime Janatian<sup>10,11</sup> · Ali Jahanbakhshi<sup>12</sup> · Mehdi Bagheri<sup>2</sup> · Ferhat Karaca<sup>1,13</sup> · Ali Al-Dousari<sup>14</sup> · Jong Ryeol Kim<sup>1</sup>

Received: 24 April 2023 / Accepted: 10 January 2024  
© The Author(s), under exclusive licence to Springer Nature B.V. 2024

## Abstract

The Middle East frontal sand and dust storms (SDS) occur in non-summer seasons, and represent an important phenomenon of this region's climate. Among the mentioned type, spring SDS are the most common. Trend analysis was used in the current study to investigate the spatial-temporal variability of springtime dust events in the Middle East using synoptic station observation from 2011 to 2022. The plausible changes in some controlling factors of dust activity at selected important dust sources in the Middle East were also studied during this time period. Our results showed a statistically significant spike in springtime dust events across the Middle East, particularly in May 2022. To evaluate the relative importance of controlling factors, the applied feature of importance analysis using random forest (RF) showed the higher relative importance of topsoil layer wetness, surface soil temperature, and surface wind speed in dust activity over the Middle East between 2011 and 2022. Long-term trend analysis of topsoil moisture and temperature, using the Mann-Kendall trend test, showed a decrease in soil moisture and an increase in soil temperature in some selected important dust sources in the Middle East. Moreover, our predictions using ARIMA models showed a high tendency to dust activities in selected major dust origins (domain 2 and domain 5) with a statistically significant increase ( $p$ -value < 0.05) between 2023 and 2029. Observed spatial and temporal changes within SDS hotspots can act as the first step to build up for the first time an SDS precise intensity scale, as well as establishing an SDS early warning system in future.

**Keywords** Sand and dust storms · Drought · Soil moisture · Soil temperature · Mann-Kendall trend test · ARIMA model · the Middle East

## Introduction

Arid and semi-arid areas, including the Sahara, the Middle East, and Mongolia, are the origin of sand and dust storms (SDS). More than 200–5000 million tons of mineral dust are estimated to be released annually by dust storms in Saharan Africa, the Middle East, and Asia (Rezazadeh et al. 2013). Middle East hosts the major SDS sources (hotspots), which are located in the deserts of the Arabian Peninsula, Tigris-Euphrates alluvial plains (Iran–Iraq border, Iraq, and eastern

Syria), and southeastern Iran (Hosseini Hamzeh et al. 2021; Middleton et al. 2021). The conducted studies on the frequency and distribution of Middle Eastern SDS introduced the Arabian Peninsula, one of the main dust hotspots in this area, where realizing a vast amount of particles can significantly deteriorate the air quality in both local and regional scales (Fattahi Masrouf and Rezazadeh 2022).

SDS with horizontal visibility below 1000 m is one of the important natural hazards which can seriously impact the earth's system, human health, and economy, specifically in West Asia, where their frequency and intensity vary over time and require more attention (Goudie and Middleton 2006; Halos and Mahdi 2021). They are characterized by strong winds and blowing particles over arid, semi-arid, and hyper-arid regions (Yin et al. 2021). Blowing desert dust endangers human society during its entrainment, short-range and/or long-range transport, and deposition (Middleton

---

Parya Broomandi and David Galán-Madruga are the first authors with the same authorship contribution.

✉ Jong Ryeol Kim  
jong.kim@nu.edu.kz

Extended author information available on the last page of the article

2017). Dust can negatively influence human health, wind and solar power production, oil and gas industry, transport industry, agriculture, and changes in the albedo of ice with resulting consequences on water availability and runoff (Al-Hemoud et al. 2019; Alshawaf et al. 2020; Hu et al. 2020; Khaniabadi et al. 2017; Mahmoodirad et al. 2019; Middleton et al. 2019; Papadopoulou et al. 2019; Soleimani et al. 2020). Besides, desert dust can ultimately cause flight delay or cancelation, rerouting aircrafts, and mechanical problems like corrosion of aircraft engines (Basha et al. 2019).

Due to the severe and significant impacts of sand and dust storms (SDSs), numerous studies have focused on accurately identifying and predicting SDS source areas to enhance disaster preparedness and damage prevention (Boroughani et al. 2021; Darvishi Bolorani et al. 2022; Gholami et al. 2021). SDS outbreaks depend not only on meteorological factors like wind speed, precipitation, and air temperature but also on terrestrial factors such as vegetation cover, snow cover, and soil characteristics (e.g., soil moisture, soil temperature) (Jiao et al. 2021; Papi et al. 2022). However, the integration of multiple remote sensing (RS) and meteorological data, which possess different spatial and temporal resolutions, and their application in SDS source prediction require further resolution (Rayegani et al. 2020). In this context, machine learning (ML) methods with their remarkable data integration capabilities are extensively employed in various data science fields, encompassing identification, classification, prediction, regression, and clustering (Alshammari et al. 2022; Holloway and Mengersen 2018; Liakos et al. 2018).

In recent times, ML methods have witnessed extensive utilization in SDS source prediction and susceptibility mapping. Lary et al. (2016) were among the first to demonstrate the promising potential of machine learning algorithms

(MLAs) in SDS source classification and identification (Lary et al. 2016). Subsequently, Nabavi et al. (2018) introduced five MLAs, including multilinear regression (MLR), random forest (RF), multivariate adaptive regression splines (MARS), support vector machine (SVM), and artificial neural network (ANN), for predicting aerosol optical depth (AOD) in West Asia (Nabavi et al. 2018). Gholami et al. (2020a) applied six MLAs, namely, eXtreme Gradient Boosting (XGBoost), Cubist, boosting multivariate adaptive regression splines (BMARS), adaptive network-based fuzzy inference system (ANFIS), Cforest, and Elasticnet, to explore land susceptibility to dust emissions in southeastern Iran (Gholami et al. 2020a). Additionally, Gholami et al. (2021) introduced an innovative integrated ML-based approach for generating spatial maps of dust sources and assessing the interpretability of these maps over Central Asia (Gholami et al. 2021). While ML-based methods, including deep learning (DP)-based techniques, have found increasing applications in SDS source prediction, only a few studies have specifically focused on predicting SDS sources at the event scale (Jiao et al. 2021).

Due to the fact that the Middle East has recently hosted major dust events (Al-Dousari et al. 2022; Doronzo et al. 2016), it is important to accurately analyze the spatial and temporal distribution of various types of dust events along with plausible changes in the dust sources' characteristics, which can ultimately impact the frequency and intensity of dust events. Additionally, the latest unprecedented levels of dust storms in the Middle East during the springtime (2022) can highlight the importance of further studies to dive deep into this matter (Fig. 1). Figure 1 shows captured natural-colour images with the Moderate Resolution Imaging Spectroradiometer (MODIS) instruments on NASA's Terra and Aqua satellites in late April 2022 and May 2022 over the

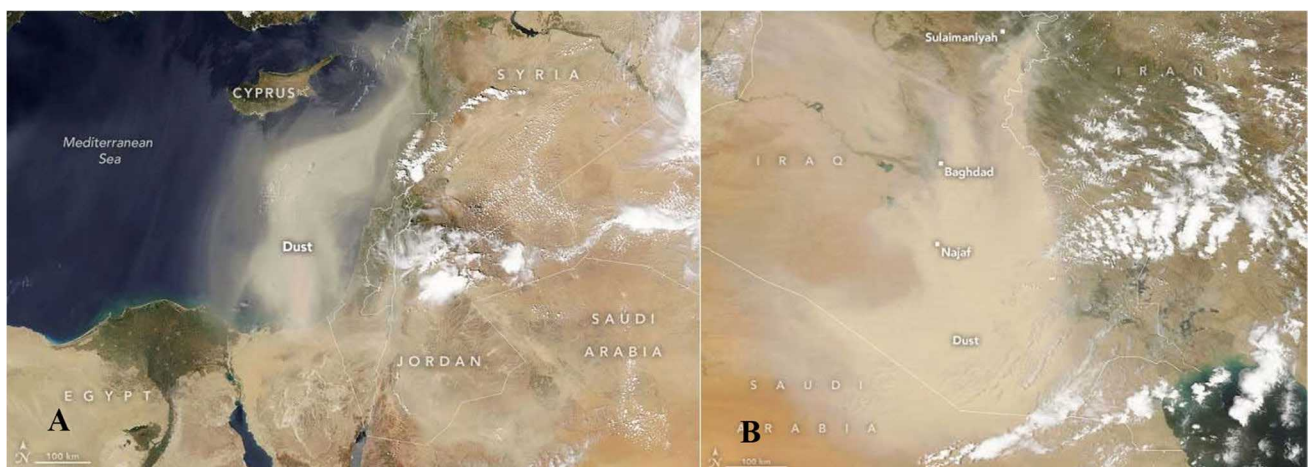


**Fig. 1** True colour image from the Aqua-MODIS sensor (<https://worldview.earthdata.nasa.gov>) on **A** 24th April 2022 and **B** 5th May 2022, focusing on the Middle East

Middle East. A thick dust cloud blanketed regions in eastern Syria, Iraq, Saudi Arabia, Kuwait, and Iran. In this period, hundreds of people were admitted to hospitals because of respiratory problems. Also, flights were grounded, and public buildings, schools, and offices were closed nationwide, and several governors declared state of emergency (Francis et al. 2022). Being continuously exposed to a thick dust blanket during springtime 2022 is quite alarming and can deeply impact societies across the region, from Syria to Iran (<https://worldview.earthdata.nasa.gov>).

It is worth mentioning that synoptic scale dust storms in the Middle East can be divided into two types: summer Shamal and frontal dust storms. Wilkerson (1991) divided frontal dust storms into two categories, postfrontal and prefrontal, which can occur at different times and places depending on the location of the front and the cyclone path. During prefrontal dust storms, the polar jet (PJ) behind and the subtropical jet (STJ) ahead of the front merge into a single jet maximum, resulting in a strong southerly to south-westerly near-surface wind. The large pressure gradient behind cold fronts causes postfrontal dust storms, also known as winter Shamal, which are directly related to eastward moving mid-latitude disturbances (Hamidi 2019; Wilkerson 1991).

The summer Shamal dust storms have received a great deal of attention; however, the frontal dust storms, which occur in non-summer seasons and are more intense than their Shamal counterpart, require more investigation (Gholamzade Ledari et al. 2020; Hamidi 2019; Hamzeh et al. 2021a; Niroomand et al. 2020; Vishkaee et al. 2011). Also, in recent years, this region has experienced some abnormalities in dust storm activities, especially during springtime, and this trend is changing into the main socio-environmental problem in the area (Khoshakhlagh et al. 2012; Mashat et al. 2020). Therefore, the aim of the current study is to delineate the spatial-temporal distribution of different types of springtime dust events for 12 years from 2011 to 2022 in the Middle East. Also, to detect the possible changes in the soil properties and meteorological parameters over major dust sources between 2011 and 2022. Besides, the dust loads from selected dust origins were predicted by ARIMA models between 2023 and 2029.

## Material and methods

### Study area

The study area is geographically between 10–45°N and 20–70°E, which covers 13 countries (Bahrain, Egypt, Iraq, Iran, Jordan, Kuwait, Lebanon, Oman, Qatar, Syria, Saudi Arabia, Turkey, and the United Arab Emirates) (Fig. 2). The arid climate, rough topography, low annual precipitation, scarcity of vegetation, and extensive sandy and clay

areas all influence dust activity in the area. In this area, dust storms occur mainly under the influence of northern winds, particularly during spring, summer, and late winter. Five important dust sources which mainly influence non-summer season dust storms in the Middle East were selected to study the plausible changes in meteorological parameters and soil characteristics, including domain 1 (D1), domain 2 (D2), domain 3 (D3), domain 4 (D4), and domain 5 (D5) (Fig. 2). D1 and D5 cover the Tigris and Euphrates alluvial plain dust sources in Iraq, local deserts, and dry wetlands in southwest Iran, Kuwait, and northern Saudi Arabia dust sources. D3 includes Syria, western Iraq, eastern Jordan, and northern Saudi Arabia dust sources. D2 and D4 contain the western, central, and eastern parts of Saudi Arabian active dust sources, respectively (Gholamzade Ledari et al. 2020; Ginoux et al. 2012; Hamidi 2019; Ledari et al. 2022).

### Ground observations

The current study obtained ground-based hourly horizontal visibility data from Iowa Environmental Mesonet (<https://www.iastate.edu/>). The hourly horizontal visibility data obtained from Iowa Environmental Mesonet were used to identify and classify dust storms in the Middle East in 179 meteorological stations between 2011 and 2022. The dust storm events were identified based on the synoptic codes presented by the World Meteorological Organisation (WMO) with horizontal visibility of fewer than 10 km. Accordingly, they are classified into three different categories: (1) severe dust storms with horizontal visibility  $\leq 200$  m, (2) moderate dust storms with  $200 \text{ m} < \text{horizontal visibility} \leq 1 \text{ km}$ , and (3) mild dust storms with  $1 \text{ km} \leq \text{horizontal visibility}$  (Hoffmann et al. 2008).

### Satellite remote sensing products

To study the plausible changes of meteorological parameters and soil characteristics in more persistent dust sources, monthly databases (<http://giovanni.sci.gsfc.nasa.gov>) of MERRA-2, GLDAS, FLDAS, and MODIS Terra were used to investigate 2-m temperature (spatial resolution of  $0.5^\circ \times 0.625^\circ$ ), surface wind speed (spatial resolution of  $0.5^\circ \times 0.625^\circ$ ) total precipitation rate (spatial resolution of  $0.25^\circ \times 0.25^\circ$ ), soil moisture content and soil temperature at 0–10 cm underground (spatial resolution of  $0.1^\circ \times 0.1^\circ$ ), and NDVI (spatial resolution of  $0.05^\circ \times 0.05^\circ$ ), between 2012 and 2022, respectively. The spring season began in March and lasted until the end of May in the current study. Also, the monthly average aerosol optical depth (AOD) of 550 nm (deep blue, land-only) from MODIS Terra (spatial resolution of  $1^\circ \times 1^\circ$ ) was used to study the changes in the dust activity over the Middle East. To investigate the dust activity over



**Fig. 2** The investigated domain in the current study. D1–D5 areas represent some selected important dust origins in the Middle East

selected major dust origins, the MODIS AOD is multiplied by an empirical coefficient of  $1.8 \text{ g m}^{-2}$  to present dust loads from the aforementioned areas (Hamidi et al. 2017).

### Evaluating springtime dust storm events trending in the Middle East

Broadly, the study of chronologically measured data time series provides a valuable source of information about

the underlying relationships among them and the ability to predict non-monitored periods. In this study, a trending analysis as a function of the type of dust storm (severe, moderate, or mild), which was identified based on the reduction in horizontal visibility, was performed to better interpret the events' time series in the target study domain. For that, mean annual data were employed. Firstly, the temporal 2011–2022 series was represented, and secondly, the best-fitting function type was selected among exponential,

linear, logarithmic, polynomial, potential, and moving average functions. In this case, a polynomial function (second degree) was regarded to evaluate the time series trend. On the other hand, independent samples *t*-test was conducted to identify potential differences among mean annual values of the investigated years, considering *p*-values lower than 0.05 statistically significant.

### Feature selection based on random forest analysis

The feature importance (FI) analysis was carried out via random forest to evaluate the relative importance of controlling factors of dust activity impacting dust loads in selected major Middle Eastern dust origins (Molla-Alizadeh-Zavardehi et al. 2014). Random forest represents one of the most widely utilized machine learning methods due to its exceptional predictive performance, ability to mitigate overfitting, and inherent interpretability (Breiman 2001). The algorithm's interpretability arises from its capacity to readily determine the significance of each variable in making decisions within the tree, making it a straightforward task to quantify the contribution of each variable to the overall decision. This interpretability is facilitated by the straightforward process of determining the importance of each variable in the decision-making within the tree.

FI analysis was applied for NDVI\_Terra, precipitation, soil temperature, soil wetness, surface wind speed, maximum 2-m temperature, minimum 2-m temperature, and mean 2-m temperature. RF helped in the selection of the most important predictors affecting dust activity based on a selection from 1 (highest importance) to zero (no importance).

### Time series analysis of some controlling factors of dust activity in selected major Middle Eastern dust origins

To analyse the significance of trends in long-term changes in controlling factors, the Mann-Kendall test (“wq” package in R) was applied, using the “seaKen” functions, for the seasonal Mann–Kendall trend tests (Kendall 1949; Mann 1945). Moreover, the Sen's Slope estimator was also applied, from the same package (wq), to quantify the magnitude of changes (Shafiee et al., 2019, 2017; Silva Junior et al. 2018).

### Autoregressive integrated moving average (ARIMA) to predict dust activity

Prediction models for the phenomenon of dust storms, based on past data, help identify the main factors contributing to their occurrence in a region and the importance of each factor. One of the most important prediction models is the ARIMA time series model, which forecasts the future state

of a variable based on its current value. In this research, autoregressive integrated moving average (ARIMA) was applied to investigate and predict dust activity in selected major Middle Eastern dust origins between 2023 and 2029. The historical data we had spanned from 2011 to 2022, allowing us to utilize the ARIMA model to forecast dust loads for the time window from 2023 to 2029 (Dargahian and Doostkamian 2021; Ghosh et al. 2023; Mahendra et al. 2023).

These models have the efficient capability of generating short-term forecasts. ARIMA model is expressed as follows:

$$Y_t = \phi_0 + \phi_1 Y_{t-1} + \phi_2 Y_{t-2} + \dots + \phi_p Y_{t-p} + \varepsilon_t - \theta_1 \varepsilon_{t-1} - \dots - \theta_q \varepsilon_{t-q}$$

where  $Y_t$ ,  $\varepsilon_t$ ,  $\phi_j$ , and  $\theta_j$  are actual value, random error at  $t$ , and coefficients, respectively.  $p$  and  $q$  referred to autoregressive and moving average, respectively. Stationary is a necessary condition in ARIMA predicting model. If trend and heterogeneity is observed in the interest time series, they need to be removed and stabilize the variance before fitting the model (Box and Jenkins 1970).

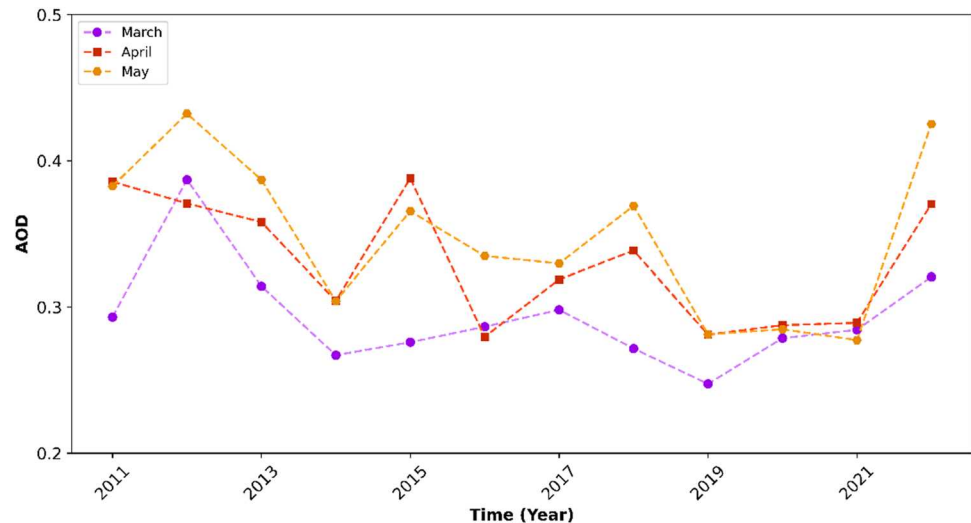
## Results

Figure 3 presents the monthly springtime time series of average aerosol optical depth 550 nm (deep blue, land-only) over the Middle East between 2011 and 2022. It shows a spike in dust activity in 2022, specifically in May (Fig. 3), following 3-year average level activities. Moreover, the monthly averaged anomalies of rainfall and soil moisture content (0–10 cm underground) showed a reduction in March, April, and May during the same period. The anomalies of soil moisture content and rainfall had a strong positive correlation ( $R^2 = 0.85$ ,  $p$ -value < 0.05). To dive deep into this matter, the current study investigated the changes in the ground-based horizontal visibility caused by the detected spike in dust activities along with the plausible changes in the controlling factors of sand and dust emissions in the Middle East between 2011 and 2022.

### Long-term spatiotemporal and trend variability of dust

Table 1 presents the total frequency of three dust storm categories in the Middle East from 2011 to 2022. Over the past 12 springs, 503, 1937, and 2440 dust events were categorized as severe (horizontal visibility  $\leq 200$  m), moderated ( $200 \text{ m} < \text{horizontal visibility} \leq 1 \text{ km}$ ), and mild dust storms (horizontal visibility  $\leq 1 \text{ km}$ ), respectively. Also, 20,787 days, expressed as the total sum of days in the study area, showed events of horizontal visibility below 10 km (blowing dust, see Table 1). The highest number of springtime

**Fig. 3** Monthly average aerosol optical depth 550 nm (deep blue, land-only) over the Middle East between 2011 and 2022



**Table 1** The recorded total springtime SDS in three defined dust event categories and blowing dust frequency in the Middle Eastern meteorological stations during 2011–2022

Year	Severe dust events (number)	Moderate dust events (number)	Mild dust events (number)	Blowing dust
2011	65	256	321	1444
2012	74	376	450	3037
2013	31	141	172	2148
2014	21	99	120	1385
2015	57	128	185	1854
2016	14	72	86	1324
2017	28	133	161	1607
2018	67	163	230	1800
2019	9	98	107	1199
2020	20	88	108	1195
2021	21	75	96	1268
2022	96	308	404	2526

severe, moderate, and mild dust storms were recorded in 2022, 2012, and 2012, respectively. In contrast, the lowest number of severe, moderate, and mild dust events were in 2019, 2021, and 2016, respectively (Table 1). In our results, different dust events had a reduction trend in the studied meteorological stations after 2012, plateauing for 3 years until 2022. However, in 2022, their occurrences suddenly spiked again. According to our results, intensive severe dust storms were mainly reported in Saudi Arabia, Iran, Iraq, Kuwait, Jordan, and Egypt, with horizontal visibility below 50 m from 2011 to 2022. Among these countries, the most intense severe events were observed in Saudi Arabia, where the horizontal visibility was repeatedly almost zero.

Table 2 shows the monthly distribution of different dust storm events recorded in the meteorological stations during the studied time frame. Severe, moderate, and mild dust events had their highest frequency in May 2022, March 2012, and May 2022, with values of 59, 178, and 225 days, respectively (Table 2). The frequency of all types of dust events experienced a notable increase in May 2022 in Middle Eastern countries. The skies of many cities turned orange, the air quality degraded, and visibility dropped to a few hundred meters (<https://earthobservatory.nasa.gov/topic/natural-event>).

Beside the recorded increase in the frequency of all springtime dust events, the annual mean of the number of dust events, which could be associated with poor air quality, experienced a statistically significant increase over time. The annual mean of the number of springtime severe, moderate, and mild dust events had a statistically significant increase over time with  $R^2 = 0.75$  ( $p$ -value < 0.05), 0.74 ( $p$ -value < 0.05), and 0.72 ( $p$ -value < 0.05), respectively, during the study period.

Figure 4 shows the observed statistically significant differences between the annual mean of the number the different springtime dust events from 2011 to 2022. Our results also revealed that the annual mean number of the springtime dust events experienced statistically significant changes between these 12 years (Fig. 4; Table 2). Compared to previous years, the number of different dust events was statistically increased in 2022. Substantial differences in 2022 (increasing) were seen in the number of mild and blowing dust events compared to other years. The number of severe dust events also had a statistically significant increase in 2022 compared to 2013, 2014, 2016, 2017, 2019, 2020, and 2021 (Fig. 4; Table 2).

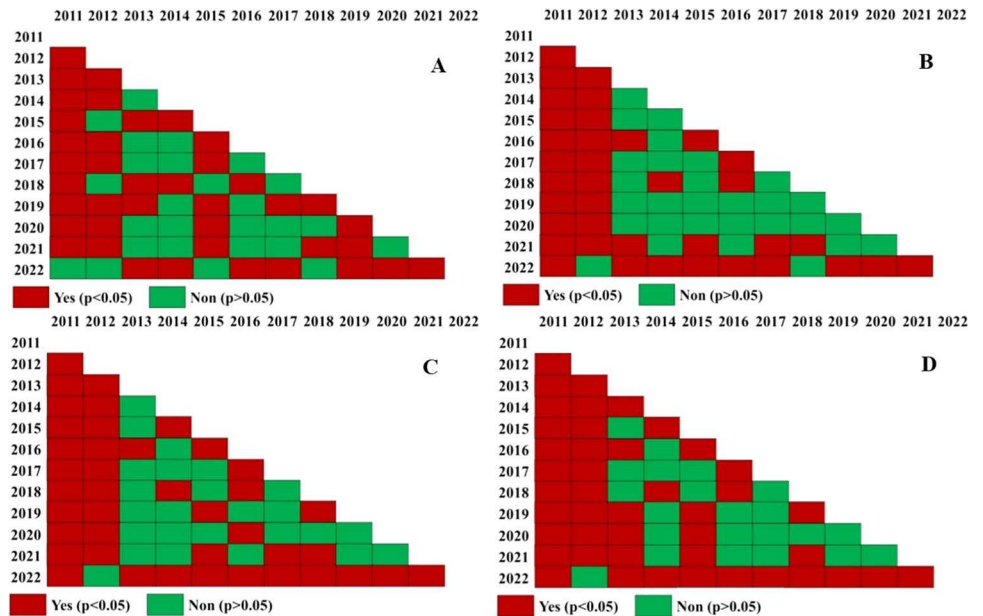
**Table 2** The recorded monthly dust storms in four defined categories in the Middle Eastern meteorological stations during 2011–2022

<i>Severe dust storm</i>				<i>Moderate dust storm</i>			
Year	March	April	May	Year	March	April	May
2011	15	33	17	2011	73	108	75
2012	38	17	19	2012	178	81	117
2013	11	7	13	2013	34	65	42
2014	6	5	10	2014	36	27	36
2015	7	37	13	2015	24	65	39
2016	0	10	4	2016	21	24	27
2017	12	6	10	2017	57	37	39
2018	11	33	23	2018	46	61	56
2019	3	2	4	2019	42	32	24
2020	5	5	10	2020	31	26	31
2021	16	2	3	2021	44	17	14
2022	15	22	59	2022	66	76	166

<i>Mild dust storm</i>				<i>Blowing dust</i>			
Year	March	April	May	Year	March	April	May
2011	88	141	92	2011	389	556	499
2012	216	98	136	2012	1168	810	1059
2013	45	72	55	2013	764	643	741
2014	42	32	46	2014	502	414	469
2015	31	102	52	2015	441	849	564
2016	21	34	31	2016	488	345	491
2017	69	43	49	2017	574	532	501
2018	57	94	79	2018	529	609	662
2019	45	34	28	2019	448	329	431
2020	36	31	41	2020	501	364	330
2021	60	19	17	2021	649	346	273
2022	81	98	225	2022	726	797	1003

**Fig. 4** The observed statistically significant differences between the annual mean durations of springtime **A** severe dust events, **B** moderate dust events, **C** mild dust events, and **D** blowing dust and time between 2011 and 2022 in the Middle East



The Pearson correlation coefficients between different dust events and time were calculated (Fig. 5). Tables 3 and 4 present the highest estimated positive and/or negative values with time between 2011 and 2022 in the Middle Eastern meteorological stations. The strongest positive correlation between time and severe, moderate, and mild dust storm events were in stations of King Khalid (Saudi Arabia,  $> +0.70$ ), Sabzevar (Iran,  $> +0.80$ ), and

Sabzevar (Iran,  $> +0.80$ ), respectively (Table 3), while meteorological stations of Jask (Iran,  $< -0.70$ ) and Mardin (Turkey,  $< -0.80$ ) had the highest negative correlation with time regarding severe, moderate, and mild dust storm events, respectively (Table 4). There are also some meteorological stations with correlation values near zero, showing neither positive nor negative correlation with time, which means there were no changes in the frequency

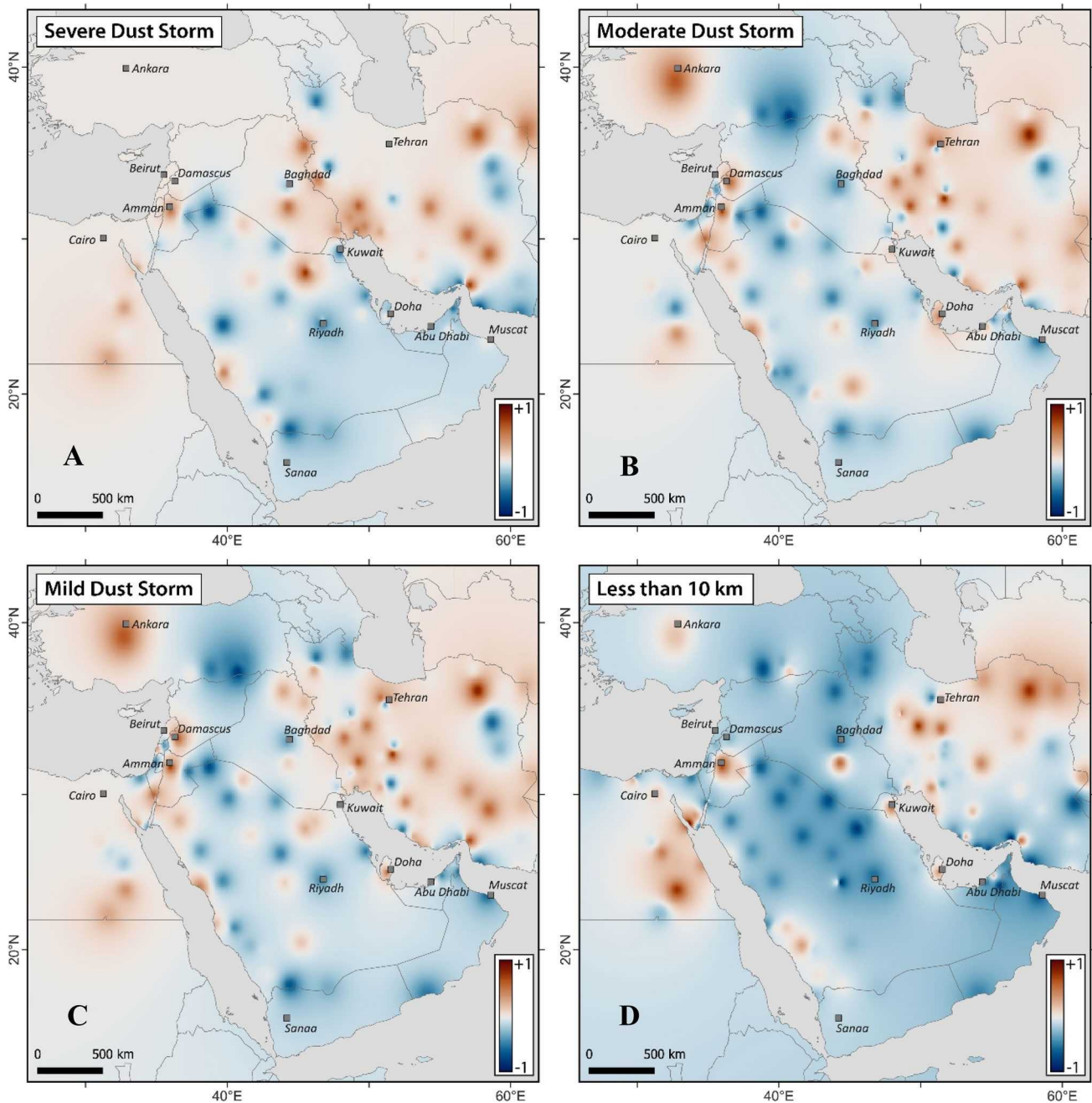


**Fig. 5** The spatial distribution of correlation strength between time and the SDS frequency of **A** severe SDS, **B** moderate SDS, **C** mild SDS, and **D** blowing dust with horizontal visibility of less than 10 km across the Middle East between 2013 and 2019



**Table 3** Some selected meteorological stations with the highest estimated positive Pearson correlation coefficient between the frequency of different dust events and time between 2011 and 2022 in the Middle East

Station	Severe dust event			Moderate dust event			Mild dust event			Blowing dust		
	Country	Station	Country	Country	Station	Country	Country	Station	Country	Country	Station	Country
King Khalid	Saudi Arabia	Sabzevar	Iran	Iran	Sabzevar	Iran	Iran	0.81	El-tor	Egypt	0.93	
Minab	Iran	Esfahan	Iran	Iran	Amman	Jordan	Jordan	0.76	Sabzevar	Iran	0.76	
Sabzevar	Iran	Amman	Jordan	Jordan	Esfahan	Iran	Iran	0.74	Arak	Iran	0.74	
Masjed Soleiman	Iran	Masjed Soleiman	Iran	Iran	Minab	Iran	Iran	0.66	Aswan	Egypt	0.74	
Bam	Iran	Cizre	Turkey	Turkey	Masjed Soleiman	Iran	Iran	0.62	Amman	Jordan	0.67	
Sulaymaniyah	Iraq	Minab	Iran	Iran	Cizre	Turkey	Turkey	0.61	Doha	Qatar	0.62	
Najaf	Iraq	Teheran	Iran	Iran	Doha	Qatar	Qatar	0.55	Amman	Jordan	0.55	
Kerman	Iran	Damascus	Syria	Syria	Bam	Iran	Iran	0.55	Kashan	Iran	0.53	
Sarakhs	Iran	Karaj	Iran	Iran	Damascus	Syria	Syria	0.55	Najaf	Iraq	0.51	
Amman	Jordan	Bandar Mahshahr	Iran	Iran	Karaj	Iran	Iran	0.50	Boroujerd	Iran	0.49	

**Table 4** Some selected meteorological stations with the highest estimated negative Pearson correlation coefficient between the frequency of different dust events and time between 2011 and 2022 in the Middle East

Station	Severe dust event			Moderate dust event			Mild dust event			Blowing dust		
	Country	Station	Country	Country	Station	Country	Country	Station	Country	Country	Station	Country
Jask	Iran	Mardin	Turkey	Turkey	Mardin	Turkey	Turkey	-0.81	Kish Island	Iran	-0.92	
Turaif	Saudi Arabia	Turaif	Saudi Arabia	Saudi Arabia	Turaif	Saudi Arabia	Saudi Arabia	-0.70	Bandar Abbas	Iran	-0.92	
Riyadh	Saudi Arabia	Riyadh	Saudi Arabia	Saudi Arabia	Nejran	Saudi Arabia	Saudi Arabia	-0.66	King Khalid	Saudi Arabia	-0.81	
Madinah	Saudi Arabia	Muscat	Oman	Oman	Jask	Iran	Iran	-0.62	Al Ain	United Arab Emirates	-0.81	
Nejran	Saudi Arabia	Kangan	Iran	Iran	Riyadh	Saudi Arabia	Saudi Arabia	-0.60	Jask	Iran	-0.79	
Doha	Qatar	Yasuj	Iran	Iran	Gonabad	Iran	Iran	-0.59	Bandar Lengeh	Iran	-0.71	
Bandar Abbas	Iran	Guriat	Saudi Arabia	Saudi Arabia	Muscat	Oman	Oman	-0.56	Rafha	Saudi Arabia	-0.71	
Ras Al Khaimah	United Arab Emirates	Sanliurfa	Turkey	Turkey	Fujeirah	United Arab Emirates	United Arab Emirates	-0.55	Sanliurfa	Turkey	-0.70	
Tabriz	Iran	Salalah	Oman	Oman	Tabriz	Iran	Iran	-0.54	Abumusa	Iran	-0.69	
Kuwait	Kuwait	Al-Jawf	Saudi Arabia	Saudi Arabia	Kangan	Iran	Iran	-0.54	Zahedan	Iran	-0.68	

of dust events. According to our results, meteorological stations in Iran, Iraq, Syria, and Egypt recorded the biggest positive changes over time (2011–2022) in the frequency of springtime dust events, which could be due to their proximity to the important active dust sources (Fig. 5). Surprisingly, there was an increase in dust storm frequency at most Iranian stations, with the exception of some limited ones located in the northwest of Iran.

### The relationship between dust activity and influencing parameters

In major selected Middle Eastern dust origins, RF analysis showed the critical role of soil temperature (FI = 0.26), surface wind speed (FI = 0.37), soil moisture content (FI = 0.29), soil moisture content (FI = 0.33), and soil moisture

content (FI = 0.32), influencing the seasonal changes in dust loads from D1, D2, D3, D4, and D5, respectively, between 2011 and 2022 (Fig. 6A).

Moreover, due to the essential controlling role of soil moisture content in the dust activity, RF analysis was performed between soil moisture content at 0–10 cm underground and other parameters with plausible influence on dust activity, including vegetation cover, 2-m temperature (maximum, minimum, and mean), total precipitation rate, soil temperature at 0–10 cm underground, and surface wind speed (Kim and Choi 2015; Munkhtsetseg et al. 2016; Nafarzadegan et al. 2021). RF analysis showed the critical role of soil temperature (FI = 0.31), surface wind speed (FI = 0.36), soil temperature (FI = 0.43), soil temperature (FI = 0.35), and soil temperature (FI = 0.43), influencing the seasonal changes in soil moisture content

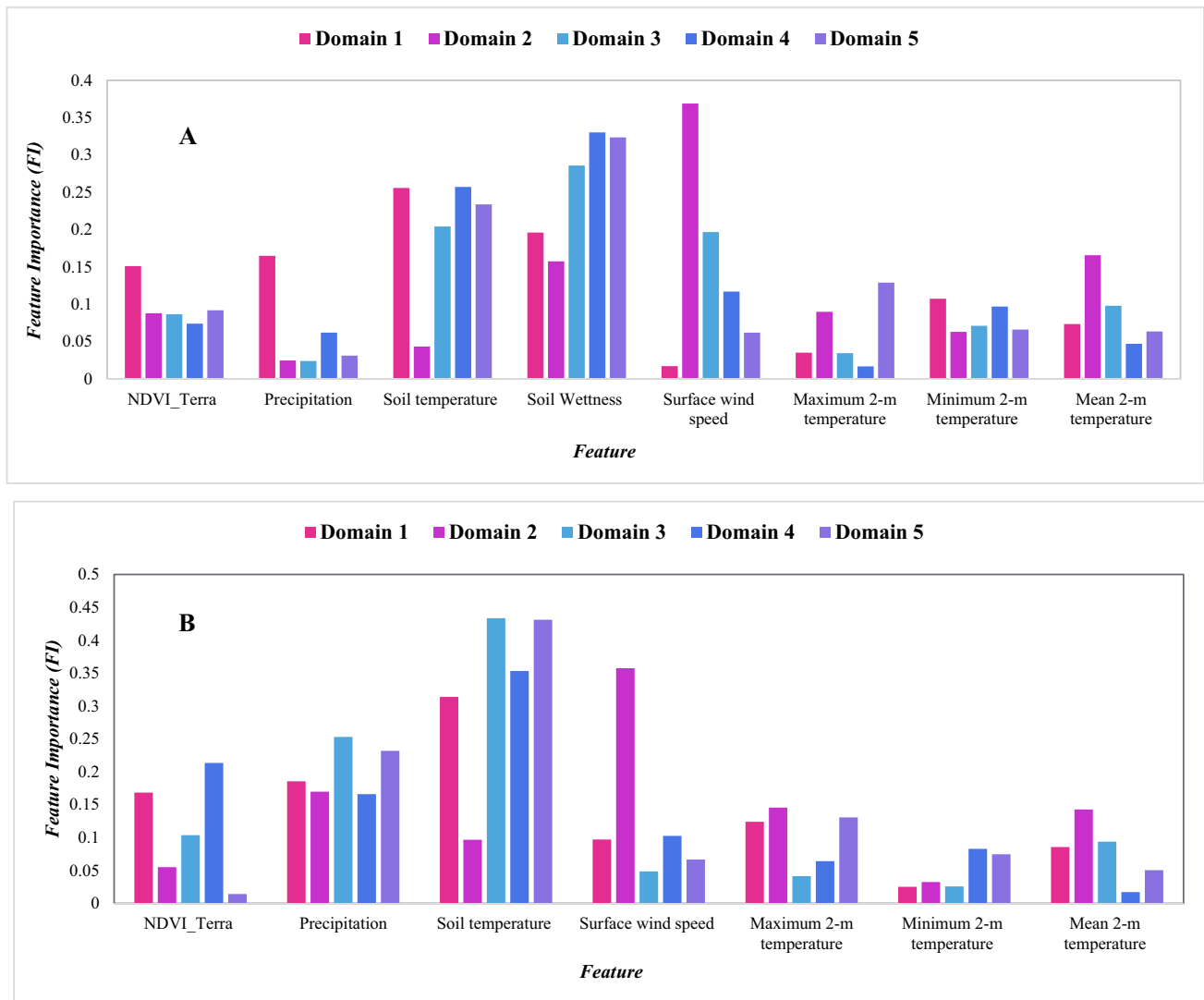


**Fig. 6** The percentages of the included features in RF, **A** dust load ( $\text{g}/\text{m}^2$ ) and **B** soil moisture content (0–10 cm underground,  $\text{m}^3/\text{m}^3$ ) wetness during studied period (2011–2022) in major dust origins of Middle East

from D1, D2, D3, D4, and D5, respectively, between 2011 and 2022 (Fig. 6B).

These results indicate a higher tendency for dust activity in the Middle East by decreases in topsoil layer wetness and an increase in surface wind speed at 2-m and surface temperature between 2011 and 2022.

### Long-term spatiotemporal and trend variability of some controlling factors of dust activity in selected major Middle Eastern dust origins

The Mann- Kendall trend test was used to investigate the spatiotemporal changes of some factors affecting the dust emission potential in selected important dust sources in the Middle East (Baghbanan et al. 2020; Kang et al. 2016). The monthly average of NDVI, soil temperature at 0–10 cm underground, soil moisture at 0–10 cm underground, total precipitation rate, 2-m temperature (maximum, mean, and minimum), and surface wind speed between 2011 and 2022 were studied here (Figs. 7, 8). Figure 7 A shows minimum NDVI values, indicating the lack of vegetation or poor vegetation cover in the study area. The highest NDVI values are only observed in Turkey, the north and northeast of Syria, the north and northeast of Iraq, and the Caspian Sea in northern Iran.

The long-term analysis of monthly NDVI\_Terra in selected important dust sources in the Middle East showed a slight reduction in the D3 and was not statistically significant ( $p$ -value  $> 0.10$ ). At the same time, NDVI had a statistically significant ( $p$ -value  $< 0.05$ ) sharp reduction in D4 between 2011 and 2022 (Table 5). Other domains (D1, D2, and D5) experienced increases in the NDVI values with the Sen's slope (magnitude of changes) of 0.0003 ( $p$ -value  $> 0.10$ ), 0.002 ( $p$ -value  $< 0.05$ ), and 0.0004 ( $p$ -value  $< 0.05$ ), respectively, in the same period.

The soil moisture (0–10 cm underground) distribution shows very low values in a large part of the studied area, mainly in Egypt, Saudi Arabia, central and southern parts of Iraq, south, and east of Lebanon, central and southwest Iran, and some parts in the southwest of Afghanistan (Fig. 7B). Despite the very low soil moisture content in vast parts of the Middle East, our analysis showed a statistically significant increase in the soil moisture levels in D1, D2, and D5 ( $p$ -value  $< 0.05$ ). Domains of D3 and D4 had a decreasing trend but were not statistically significant ( $p$ -value  $> 0.10$ ). The increasing trend of soil moisture had magnitude changes of 0.20, 0.21, and 0.10 in the D1, D2, and D5, respectively. Figure 7 C represents the soil temperature distribution in the Middle East, with its highest values in parts of Oman. The soil skin temperature is relatively high in a vast part of the study domain, but north and northwest of Iran, the Zagros Range, East of Turkey, and central Afghanistan experienced lower soil

temperature levels between 2011 and 2022 (Fig. 7C). Despite the observed increasing trend of soil moisture content, soil temperature (0–10 cm underground) had statistically significant ( $p$ -value  $< 0.05$ ) increases in domains of D1, D2, and D5 (Table 5). The remaining domains (D3 and D4) showed a decline (not statistically significant,  $p$ -value  $> 0.10$ ) in the skin soil temperature.

Figure 8 A shows the monthly averaged total precipitation rate with very low values in the vast areas of the study area. The highest values were only witnessed in Turkey, the north and northeast of Iraq, some parts of west and east of Syria, northern Iran, and the Zagros Range. Table 5 shows a general reduction in the selected dust sources in the Middle East but is statistically insignificant ( $p$ -value  $> 0.10$ ). Besides, the monthly averaged mean ambient temperature (2-m air temperature) is relatively high in many parts of the study area but not in Turkey, the north and northwest of Iran, and some parts in the northeast of Iran along with the Zagros Range (Fig. 8B). Our trend analysis showed a statistically significant increase ( $p$ -value  $< 0.05$ ) over the selected dust origins between 2011 and 2022 (Table 5).

The magnitudes of changes were 0.14, 0.09, 0.05, 0.10, and 0.11 in the D1, D2, D3, D4, and D5, respectively. The maximum and minimum air temperatures followed statistically significant increasing trends ( $p$ -value  $< 0.05$ ) in our interest dust origins (Table 5). The monthly averaged surface wind speed varies in the study area, with its highest values on the border of Iran and Afghanistan. The surface wind speed is relatively high over Saudi Arabia, north and northwest of Iraq, Egypt, and Syria (Fig. 8C). Depending on the location of dust origins, the surface wind speed followed a different change over time. The domains of D2 and D3 had an increasing trend but were not statistically significant ( $p$ -value  $> 0.10$ ) with Sen's slope of 0.01 and 0.12, respectively, while remaining domains followed statistically insignificant decreasing trends ( $p$ -value  $> 0.10$ ) (Table 5).

### Prediction of dust activity in selected major dust origins in the Middle East

The best model was fitted according to Table 6. Removal of trend and drift in the ARIMA model forecasting was achieved through the use of a constant term. To determine the presence or absence of a deterministic trend in the model, the model was initially fitted with a constant term, and then, decisions were made based on the  $t$ -statistic and  $p$ -value regarding the presence or absence of the constant term in the model. According to Table 7, the  $t$ -statistics for all domains (D1, D2, D3, D4, and D5) are less than 2, with values of 1.92, 0.59, 0.25, 1.51, and 0.95, respectively, indicating that there is no need to include the constant term in the models. The  $p$ -values for each domain are also shown to be greater than 0.05, with values of 0.084,

**Fig. 7** Time-averaged maps of **a** NDVI, **b** soil moisture content (0–10 cm underground), and **c** soil temperature (0–10 cm underground) in the Middle East between 2011 and 2022

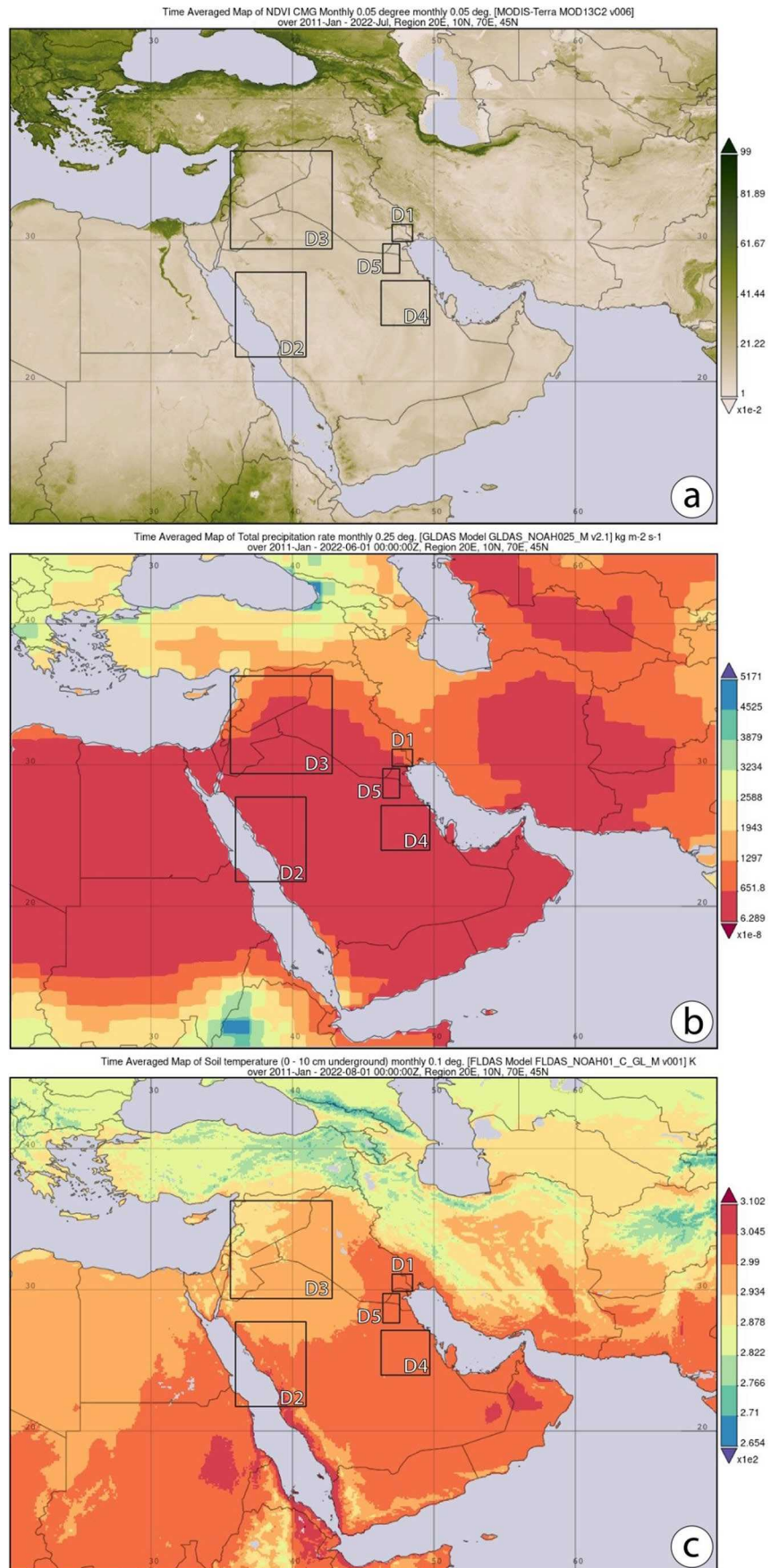


**Fig. 8** Time-averaged maps of **a** total precipitation rate, **b** 2-m air temperature, and **c** surface wind speed in the Middle East between 2011 and 2022

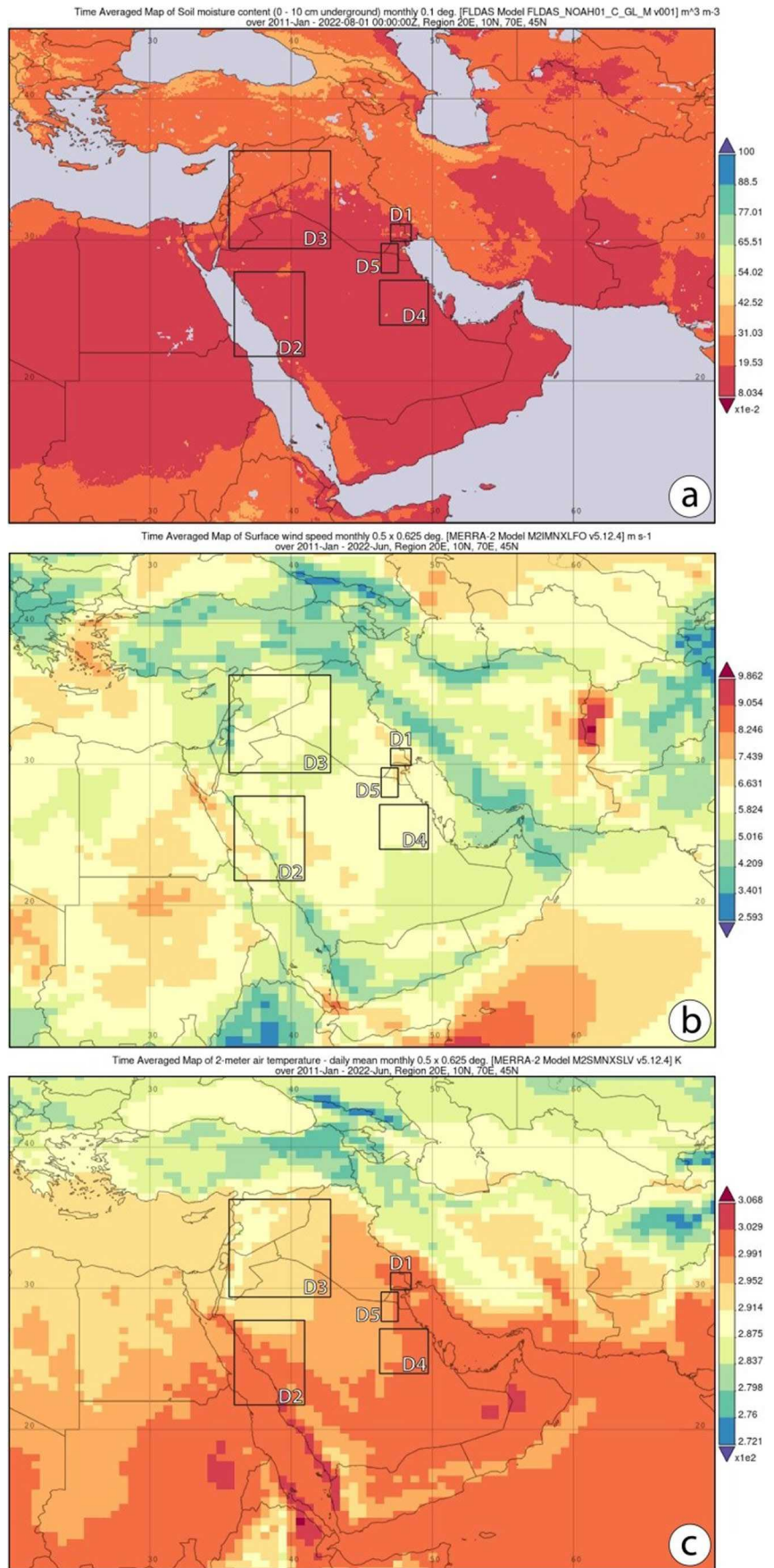


**Table 5** The observed trend of changes in some controlling factors in the selected dust origins in the Middle East between 2011 and 2022

Domain	Sen's slope	Direction	P-value	Significance
<i>NDVI_Terra</i>				
Domain 1	0.000328	Increasing	0.19562	$p > 0.10$
Domain 2	0.002059	Increasing	0.00000	$p < 0.05$
Domain 3	-0.000111	Decreasing	0.37591	$p > 0.10$
Domain 4	-0.000280	Decreasing	0.00061	$p < 0.05$
Domain 5	0.000443	Increasing	0.00117	$p < 0.05$
<i>Precipitation</i>				
Domain 1	0.000000	Decreasing	0.55325	$p > 0.10$
Domain 2	0.000000	Increasing	0.19285	$p > 0.10$
Domain 3	0.000000	Decreasing	0.28804	$p > 0.10$
Domain 4	0.000000	Decreasing	0.53449	$p > 0.10$
Domain 5	0.000000	Decreasing	0.53967	$p > 0.10$
<i>Soil temperature (0–10 cm underground)</i>				
Domain 1	0.180928	Increasing	0.00000	$p < 0.05$
Domain 2	0.206063	Increasing	0.00000	$p < 0.05$
Domain 3	-0.024672	Decreasing	0.57031	$p > 0.10$
Domain 4	-0.019200	Decreasing	0.35193	$p > 0.10$
Domain 5	0.085053	Increasing	0.00454	$p < 0.05$
<i>Soil Wetness (0–10 cm underground)</i>				
Domain 1	-0.025923	Decreasing	0.21177	$p > 0.10$
Domain 2	0.120142	Increasing	0.00601	$p < 0.05$
Domain 3	0.010911	Increasing	0.35193	$p > 0.10$
Domain 4	0.042194	Increasing	0.15262	$p > 0.10$
Domain 5	-0.006723	Decreasing	0.90962	$p > 0.10$
<i>Surface wind speed</i>				
Domain 1	-0.005235	Decreasing	0.76788	$p > 0.10$
Domain 2	0.010773	Increasing	0.51027	$p > 0.10$
Domain 3	0.012135	Increasing	0.45372	$p > 0.10$
Domain 4	-0.010747	Decreasing	0.63352	$p > 0.10$
Domain 5	-0.010939	Decreasing	0.60154	$p > 0.10$
<i>Maximum temperature at 2 m</i>				
Domain 1	0.147813	Increasing	0.00005	$p < 0.05$
Domain 2	0.111609	Increasing	0.00187	$p < 0.05$
Domain 3	0.099671	Increasing	0.01030	$p < 0.05$
Domain 4	0.123503	Increasing	0.00018	$p < 0.05$
Domain 5	0.127003	Increasing	0.00007	$p < 0.05$
<i>Minimum temperature at 2 m</i>				
Domain 1	0.136451	Increasing	0.00003	$p < 0.05$
Domain 2	0.118424	Increasing	0.00253	$p < 0.05$
Domain 3	0.106683	Increasing	0.00690	$p < 0.05$
Domain 4	0.105583	Increasing	0.00001	$p < 0.05$
Domain 5	0.143425	Increasing	0.00001	$p < 0.05$
<i>Mean temperature at 2 m</i>				
Domain 1	0.102156	Increasing	0.00187	$p < 0.05$
Domain 2	0.085438	Increasing	0.01173	$p < 0.05$
Domain 3	0.048529	Increasing	0.05363	$0.05 < p < 0.10$
Domain 4	0.095775	Increasing	0.00043	$p < 0.05$
Domain 5	0.108315	Increasing	0.00026	$p < 0.05$

**Table 6** The best selected ARIMA models in this research.

Row	Domains	Type models
1	D1	ARIMA (1,1,1)
2	D2	ARIMA (1,2,0)
3	D3	ARIMA (0,1,2)
4	D4	ARIMA (0,1,2)
5	D5	ARIMA (0,2,2)

**Table 7** The forecast variables of the selected ME dust origins in the current study

Domains	Type	Coef	SE Coef	T	P
D1	AR1	0.281	0.137	2.05	0.04
	MA1	1.06	0.039	27.26	000
	Constant	0.001	0.000	1.92	0.084
D2	AR1	-0.689	0.127	-5.40	000
	Constant	00.4	0.007	0.59	0.557
D3	MA1	0.840	0.168	4.99	0.000
	MA2	0.140	0.165	0.85	0.040
	Constant	000	000	0.25	0.806
D4	AR1	0.830	0.070	11.8	0.000
	AR2	0.274	0.099	2.79	0.009
	Constant	0.002	0.001	1.51	0.140
D5	MA1	1.487	0.001	12.5	000
	MA2	-0.394	0.783	-3.04	000
	Constant	0.001	0.001	0.95	0.352

0.555, 0.806, 0.140, and 0.352, respectively, indicating that the null hypothesis cannot be rejected, meaning there is no deterministic trend in the AOD time series models for the Middle East (Dargahian and Doostkamian 2021). In the next step, judgments are made on the model variables (AR and MA). If the  $p$ -value for any component of the fitted model is greater than 0.05, it should be reduced by one order, and the model should be refitted with the new orders. As seen in Table 7, the  $p$ -values for the model variables are less than 0.05.

The dust loads from selected domains was predicted using ARIMA models from 2023 to 2029 (Table 8). The highest tendency to dust activities was predicted in D5, while D3 showed lower activity compared to the remaining dust origins. Trend analysis using Mann-Kendall trend test showed a statistically significant increase ( $p$ -value  $< 0.05$ ) in the dust activity (dust loads) in domains of D1, D2, D4, and D5 with Sen's slope of 0.002, 0.03, 0.003, and 0.02, respectively, between 2023 and 2029. The third domain (D3) had also an increasing trend in dust activity but not statistically significant ( $p$ -value  $> 0.05$ ).

**Table 8** The predicted seasonal dust loads ( $\text{g}/\text{m}^2$ ) from selected major dust origins in the Middle East between 2023 and 2029.

Year	Domains				
	D1	D2	D3	D4	D5
2023	0.7488	0.7758	0.6606	0.8190	1.0494
2024	0.7452	0.8100	0.6498	0.8118	1.0872
2025	0.7470	0.8514	0.6498	0.8154	1.1268
2026	0.7506	0.8946	0.6498	0.8208	1.1700
2027	0.7542	0.9450	0.6498	0.8262	1.2168
2028	0.7578	0.9990	0.6498	0.8298	1.2636
2029	0.7596	1.0602	0.6516	0.8352	1.3158

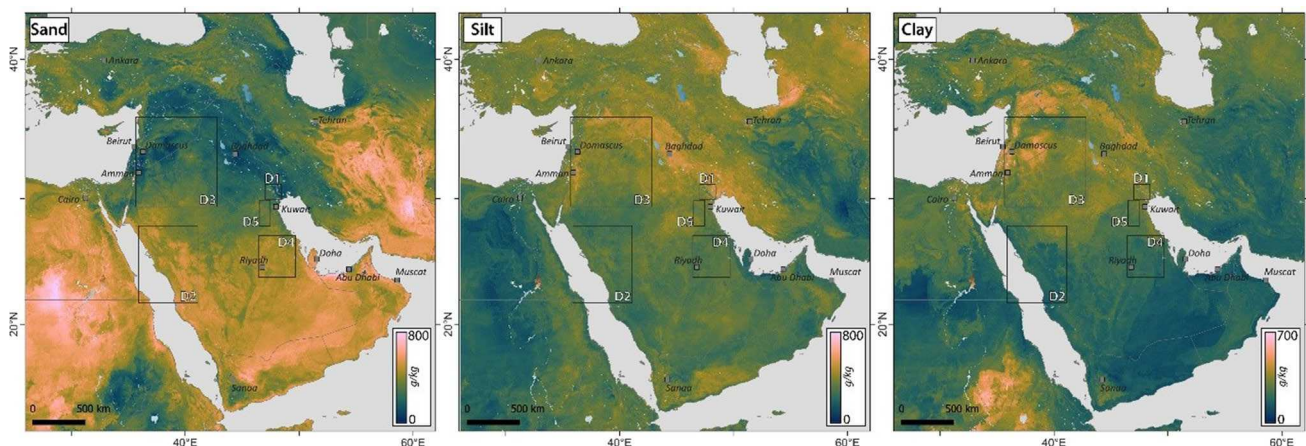
Generally, our results showed that small values of NDVI were observed in the areas with low precipitation and soil moisture content, including vast parts of Syria, Iraq, Saudi Arabia, and southwestern Iran (Figs. 7 and 8), transferring this area into a dust-prone region. Most parts of the Middle East consist of arid and semi-arid lands and deserted areas containing soil particles with different size distributions (Fig. 9). At the same time, they are active sources of atmospheric dust. In our selected dust sources, D3, D1, and D5 mainly contain silt and clay, while D2 and D4 mainly consist of sandy soil particles, which can lead to the transportation of large particles to the downwind areas. According to our findings, D1 and D5 with higher content of silt and clay, compared to other selected dust sources, experienced statistically significant changes over time in ambient temperature (increasing), total precipitation rate (decreasing), surface soil temperature (increasing), and surface soil wetness (decreasing but not statistically significant in D1). Increasing concerns about potential increases in atmospheric dust concentrations are attributed to these active dust sources.

## Discussion

After having a low-level trend for 3 years, the detected spike, which occurred in 2022 springtime dust events, specifically in May 2022, could be attributed to the fluctuations in climate which may happen in decades, or an extreme weather event observed in this particular year (Fattahi Masrouf and Rezazadeh 2022; Francis et al. 2022). Also, these changes could have impacts on the soil characteristics, i.e., soil moisture in the arid and semi-arid areas of the Middle East. It may be also speculated that it is an impact of changing climate, but its confirmation requires a longer-term investigation in the future.

Extreme variations in climate, which can be linked to climate change, and consequently changes in the arid and semi-arid areas are vital controlling factors in the dust emission potential, the frequency and intensity of SDS events, and the movement of dust storms (Hamidi and Roshani 2023; Modarres 2021).

Numerous environmental, geographic, and bioclimatic factors, such as soil properties, digital elevation models (DEM), topographic characteristics, vegetation cover, land surface roughness, wind conditions, precipitation, and slope, collectively influence dust sources or emissions from land surfaces (Gholami and Mohammadifar 2022). Among influencing meteorological parameters, changes in precipitation inversely impact the frequency and intensity of dust events, while wind speed and temperature variations directly impact it (Hamzeh et al. 2021b; Hossein Hamzeh et al. 2021; Karami et al. 2021; Namdari et al. 2018). The overall detected reduction in the total precipitation rate, along with increased air temperature and surface wind speed in the selected dust origins, could be attributed to the same extremities observed in the Middle East. Moreover, increased ambient air temperature can also decrease the required threshold wind speed

**Fig. 9** The particle size distribution over the study domain (<https://soilgrids.org/>)

in dust emission initiation by reducing the relative humidity (Broomandi et al. 2021; Gholami et al. 2020b; Molla-Alizadeh-Zavardehi et al. 2014; Namdari et al. 2018). A recently conducted study, by applying Dragonfy algorithm (DA) showed that features of DEM or elevation, land use, clay content, silt content, precipitation, soil bulk density, and wind speed were deemed significant in controlling ME dust sources (Gholami and Mohammadifar 2022). In their study, the relative importance and contribution of the key variables influencing dust sources were assessed using game theory. Out of the seven crucial features selected by DA, three variables, namely, clay content, silt content, and precipitation, obtained the highest importance scores. Based on the permutation values, these three variables were found to have the most significant impact on the model output, indicating their critical role in controlling dust emissions. Overall, pedoclimatic variables, land surface conditions, and roughness emerged as the essential factors governing wind erosion and dust emissions (Gholami and Mohammadifar 2022). Moreover, in Central Asia, the three most critical variables controlling dust sources are precipitation, soil bulk density, and slope. Additionally, in the Sistan basin, the essential variables controlling dust sources are wind speed, elevation, and soil organic carbon, all identified through a genetic algorithm (Gholami et al. 2020b).

It is worth mentioning that not only fluctuations in climate are responsible for the growing trend of SDS events over the Middle East, but anthropogenic activities are as well. Human activities such as drying rivers and lakes, land-use changes, poor management of water resources, dam construction projects in adjoining countries, the political instability causing military operations and war impacts, and deforestation have an important role in emerging the SDS events in the region (Al-Dousari et al. 2018; Attiya and Jones 2020; Hamidi 2020; Ledari et al. 2022; Mahmoodirad and Sanei 2015).

Apart from the variables mentioned above, topsoil layer wetness (soil moisture content at 0–10 cm underground) is an important factor in estimating the potential of sand and dust emission. The soil moisture can enhance the strength of inter-particle bonds by developing a sticky film between particles and result in suppressing dust emission. However, the topsoil layer wetness strongly depends on surface temperature (soil temperature at 0–10 cm underground) and will be decreased by surface temperature increment and this could result in the increase of dust emission potential (Broomandi et al. 2021). Hence, it can be said that since wind erosion prevailed by the real surface soil wetness, any variation in both temporal and spatial scale can influence the tendency for dust emission. The observed decreasing trend in the topsoil layer wetness in association with the increasing trend of topsoil temperature in some selected important dust sources over the studied period can be a severe and alarming issue

and reason for the future unprecedented levels of dust storms in the Middle East (Darvishi Boloorani et al. 2014; Mehrizi 2020; Mohammadpour et al. 2020; Yin et al. 2021).

The direct and indirect adverse impacts of dust events show the necessity of taking effective functional stabilizing techniques to mitigate wind erosion, developing suitable climate adaption and mitigation strategies, developing a more reliable and accurate early warning system, and quantifying the impacts on societal implications on both national and regional scales. Due to the nature of this natural hazard, it is important to build science-based national, regional, and international partnerships to combat SDS events in source areas and also impacted regions. A transboundary multi-hazard risk assessment is important in analysing the cause-and-effect relationships and helping policymakers fully understand the required dynamics and complexity of policy actions. Such a transboundary dialogue and collaboration between affected counties (SDS sources and impacted areas) lead to policy interventions reflecting the geospatial link among origins and receptors, which can positively influence adaption and mitigation aspects (Orlovsky et al. 2013).

## Conclusion

The present study investigated the spatial and temporal variation of springtime dust events, including severe, moderate, and mild dust storms, in the Middle East from 2011 to 2022. The Mann-Kendall trend test was deployed to investigate the long-term changes in meteorological parameters (including 2-m temperature, total precipitation rate, and surface wind speed) and soil properties (including soil moisture and temperature at 0–10 cm underground and NDVI) using satellite products over the studied time period in selected Middle Eastern important dust sources. According to our results, there was a spike in the frequency of all types of dust events in the Middle Eastern meteorological stations in 2022, particularly in May, compared to the previous years.

RF analysis indicated a higher tendency for dust activity in the Middle East by decreases in topsoil layer wetness and an increase in surface wind speed at 2-m and surface temperature between 2011 and 2022. Mann-Kendall trend analysis showed a reduction in the NDVI values and soil moisture content (0–10 cm underground), over D3 ( $p$ -value  $> 0.10$ ) and D4 ( $p$ -value  $< 0.05$ ), and D1 ( $p$ -value  $> 0.10$ ) and D5 ( $p$ -value  $> 0.10$ ), respectively, between 2011 and 2021, while soil temperature (0–10 cm underground) experienced a statistically significant increasing trend ( $p$ -value  $< 0.05$ ) in domains of D1, D2, and D5. Moreover, our predictions using ARIMA models showed the highest tendency to dust activities in D2 and D5 with a statistically significant increase ( $p$ -value  $< 0.05$ ) between 2023 and 2029.



Although the trends indicate an increase in dust activity in the Middle East, there are some differences between the trends of the investigated selected regions. These differences could be due to the effect of climate change on the areas and also the political and economic conditions of related countries. In other words, according to the political stability and suitable economic situation of some countries in the Middle East area, they had adequate financial support and enough concentration for focusing on dust emission suppressing projects in their local dust sources, and this could result in controlling the dust emission in their area and as a consequence decrease the effect of climate change on intensification of dust events in their countries.

It can also be concluded that the observed increasing trend in the frequency and intensity of different dust events in affected meteorological stations along with alarming changes over important dust sources in the Middle East requires effective international collaborations to combat, control, manage, and minimize the catastrophic dust events.

Moreover, due to the numerous advantages of machine learning, such as its potential for monitoring natural hazards, providing early warnings, and supporting sustainable land management, it can be a promising approach for future studies to address challenges related to dust storms, including classification and prediction based on satellite images or meteorological data analysis. Upon examining existing applications of machine learning in dust storm prediction, it is evident that most studies have focused on daily predictions and real-time detection. There is room for further research to extend the prediction horizon beyond three days. Additionally, there is an opportunity to use machine learning to forecast specific dust storm characteristics, such as duration and intensity, which are crucial for effective warning systems.

Addressing the spatial or temporal limitations of available data could be achieved through the integration of various data sources, such as regional-scale meteorological data providing surface-level atmospheric measurements and remote sensing images covering larger areas. Combining object detection techniques with meteorological data, such as wind speed, direction, and air quality measurements, may improve the ability to distinguish dust, clouds, and ice. It is recommended to adopt deep learning models, as they excel at detecting complex patterns in processing time series data which could lead to improved prediction performance. To further advance research in this area, investigations into dust storm emissions, transport, and depositions are also needed. Additionally, exploring the potential benefits of novel deep learning models can help enhance the understanding and prediction of dust storms.

**Supplementary Information** The online version contains supplementary material available at <https://doi.org/10.1007/s11869-024-01510-9>.

**Author contribution** Parya Broomandi: supervision, writing — original draft, conceptualization, methodology, validation, formal analysis, investigation, data curation. David Galán-Madruga: methodology, data analysis, data curation, formal analysis, review and editing. Alfreido Satyanaga: resources, data curation, data analysis, investigation, project administration, funding acquisition, review and editing. Mehdi Hamidi: data curation, validation, review and editing. Dorna Gholamzade Ledari: conceptualization, methodology, writing — original draft, data curation. Aram Fathian: conceptualization, methodology, data curation, formal analysis. Rasoul Sarvestan: data analysis, data curation. Nasime Janatian: data analysis, data curation. Ali Jahanbakhshi: data analysis, data curation. Mehdi Bagheri: resources, data curation, project administration, funding acquisition. Ferhat Karaca: methodology, validation, review and editing. Ali Al-Dousari: supervision, validation, review and editing. Jong Ryeol Kim: resources, data curation, project administration, funding acquisition.

**Funding** The authors acknowledge the financial support provided in part by the Faculty Development Competitive Research Grant (FDCRG), Nazarbayev University (Project No. 201223FD8811) and the Collaborative Research Project (CRP) grant, Nazarbayev University (Project No. 11022021CRP1512).

**Data availability** Data is available on request from the authors.

## Declarations

**Ethics approval** Not applicable.

**Consent to participate** Not applicable.

**Consent for publication** Not applicable.

**Conflict of interest** The authors declare no competing interests.

## References

- Al-Dousari A, Omar A, Al-Hemoud A, Aba A, Alrashedi M, Alrawi M et al (2022) A success story in controlling sand and dust storms hotspots in the middle east. *Atmosphere* 13:8. <https://doi.org/10.3390/atmos13081335>
- Al-Dousari AM, Ibrahim MI, Al-Dousari N, Ahmed M, Al-Awadhi S (2018) Pollen in aeolian dust with relation to allergy and asthma in Kuwait. *Aerobiologia* 34:325–336. <https://doi.org/10.1007/s10453-018-9516-8>
- Al-Hemoud A, Al-Dousari A, Misak R, Al-Sudairawi M, Naseeb A, Al-Dashti H, Al-Dousari N (2019) Economic impact and risk assessment of sand and dust storms (SDS) on the oil and gas industry in Kuwait. *Sustainability* 11:1–19. <https://doi.org/10.3390/su11010200>
- Alshammari RK, Alrwais O, Aksoy MS (2022) Machine learning applications to dust storms: a meta-analysis. *Aerosol Air Qual Res* 22:220183. <https://doi.org/10.4209/aaqr.220183>
- Alshawaf M, Poudineh R, Alhajeri N (2020) Solar PV in Kuwait: The effect of ambient temperature and sandstorms on output variability and uncertainty. *Renew Sust Energ Rev* 134:110346. <https://doi.org/10.1016/j.rser.2020.110346>
- Attiya A, Jones B (2020) Climatology of Iraqi dust events during 1980–2015. *SN Appl Sci* 2. <https://doi.org/10.1007/s42452-020-2669-4>
- Baghbanan P, Ghavidel Y, Farajzadeh M (2020) Spatial analysis of spring dust storms hazard in Iran. *Theor Appl Climatol* 139:1447–1457. <https://doi.org/10.1007/s00704-019-03060-y>

- Basha G, Ratnam MV, Kumar KN, Ouarda TB MJ, Kishore P, Velicogna I (2019) Long-term variation of dust episodes over the United Arab Emirates. *J Atmos Sol-Terr Phys* 187:33–39. <https://doi.org/10.1016/j.jastp.2019.03.006>
- Boroughani M, Pourhashemi S, Gholami H, Kaskaoutis DG (2021) Predicting of dust storm source by combining remote sensing, statistic-based predictive models and game theory in the Sistan watershed, southwestern Asia. *J Arid Land* 13:1103–1121. <https://doi.org/10.1007/s40333-021-0023-3>
- Box G, Jenkins G (1970) Time series analysis: forecasting and control. Holden-Day, San Francisco
- Breiman L (2001) Random forests. *Mach Learn* 45:5–32. <https://doi.org/10.1023/A:1010933404324>
- Broomandi P, Karaca F, Guney M, Fathian A, Geng X, Kim JR (2021) Destinations frequently impacted by dust storms originating from southwest Iran. *Atmos Res* 248:105264. <https://doi.org/10.1016/j.atmosres.2020.105264>
- Dargahian F, Doostkamian M (2021) Assessment and forecasting spatial pattern changes of dust and wind speed using ARIMA and ANNs model in Helmand Basin, Iran. *J Earth Syst Sci* 130:114. <https://doi.org/10.1007/s12040-021-01613-2>
- Darvishi Boloorani A, Nabavi SO, Bahrami H, Mirzapour F, Kavosi M, Abbasi E, Azizi R (2014) Investigation of dust storms entering western Iran using remotely sensed data and synoptic analysis. *Iranian J Environ Health Sci Eng* 12. <https://doi.org/10.1186/s40201-014-0124-4>
- Darvishi Boloorani A, Neysani Samany N, Papi R, Soleimani M (2022) Dust source susceptibility mapping in Tigris and Euphrates basin using remotely sensed imagery. *Catena* 209:105795. <https://doi.org/10.1016/j.catena.2021.105795>
- Doronzo DM, Al-Dousari AM, Folch A, Waldhauserova PD (2016) Preface to the dust topical collection. *Arab J Geosci* 9:468. <https://doi.org/10.1007/s12517-016-2504-9>
- Fattahi Masrouf P, Rezazadeh M (2022) Spatio-temporal distribution of various types of dust events in the Middle East during the period 1996–2015. *J Earth Sp Phys* 47:231–248. <https://doi.org/10.22059/jesphys.2021.321010.1007306>
- Francis D, Fonseca R, Narendra Reddy N, Bozkurt D, Cuesta J, Bosc E (2022) On the Middle East's severe dust storms in spring 2022: triggers and impacts. *Atmos Environ* 296. <https://doi.org/10.1016/j.atmosenv.2022.119539>
- Gholami H, Mohamadifar A, Malakooti H, Esmaeilpour Y, Golzari S, Mohammadi F, Li Y, Song Y, Kaskaoutis D, Fitzsimmons K, Collins A (2021) Integrated modelling for mapping spatial sources of dust in central Asia — an important dust source in the global atmospheric system. *Atmos Pollut Res*. <https://doi.org/10.1016/j.apr.2021.101173>
- Gholami H, Mohamadifar A, Sorooshian A, Jansen JD (2020a) Machine-learning algorithms for predicting land susceptibility to dust emissions: the case of the Jazmurian Basin, Iran. *Atmos Pollut Res* 11:1303–1315. <https://doi.org/10.1016/j.apr.2020.05.009>
- Gholami H, Mohammadifar A (2022) Novel deep learning hybrid models (CNN-GRU and DLDL-RF) for the susceptibility classification of dust sources in the Middle East: a global source. *Sci Rep* 12:19342. <https://doi.org/10.1038/s41598-022-24036-5>
- Gholami H, Rahimi S, Fathabadi A, Habibi S, Collins A (2020b) Mapping the spatial sources of atmospheric dust using GLUE and Monte Carlo simulation. *Sci Total Environ* 723. <https://doi.org/10.1016/j.scitotenv.2020.138090>
- Gholamzade Ledari D, Hamidi M, Shao Y (2020) Evaluation of the 13 April 2011 frontal dust storm in west Asia. *Aeolian Res* 44:100592. <https://doi.org/10.1016/j.aeolia.2020.100592>
- Ghosh AK, Das S, Dutta S, Mukherjee A (2023) Sensing of particulate matter (PM 2.5 and PM 10) in the air of tier 1, tier 2, and tier 3 cities in India using EVDHM-ARIMA hybrid model. *IEEE Sens Lett* 7:1–4. <https://doi.org/10.1109/LENS.2023.3270905>
- Ginoux P, Prospero J, Gill T, Hsu N, Zhao M (2012) Global-scale attribution of anthropogenic and natural dust sources and their emission rates based on MODIS Deep Blue aerosol products. *Rev Geophys* 50:3005. <https://doi.org/10.1029/2012RG000388>
- Goudie A, Middleton N (2006) Desert dust in the global system. *Desert Dust Glob Syst*:1–287. <https://doi.org/10.1007/3-540-32355-4>
- Halos SH, Mahdi S (2021) Effect of climate change on spring massive sand/dust storms in Iraq. *Al-Mustansiriyah J Sci* 32:13–20. <https://doi.org/10.23851/mjs.v32i4.1105>
- Hamidi M (2019) Atmospheric investigation of frontal dust storms in Southwest Asia. *Asia Pac J Atmos Sci* 55:177–193. <https://doi.org/10.1007/s13143-018-0083-2>
- Hamidi M (2020) The key role of water resources management in the Middle East dust events. *Catena* 187:104337. <https://doi.org/10.1016/j.catena.2019.104337>
- Hamidi M, Kavianpour MR, Shao YP (2017) A quantitative evaluation of the 3–8 July 2009 Shamal dust storm. *Aeolian Res* 24:133–143. <https://doi.org/10.1016/j.aeolia.2016.12.004> 5308P. JIAO ET AL
- Hamidi M, Roshani A (2023) Investigation of climate change effects on Iraq dust activity using LSTM. *Atmos Pollut Res*:101874. <https://doi.org/10.1016/j.apr.2023.101874>
- Hamzeh NH, Karami S, Opp C, Fattahi E, Jean-François V (2021a) Spatial and temporal variability in dust storms in the Middle East, 2002–2018: three case studies in July 2009. *Arab J Geosci* 14:538. <https://doi.org/10.1007/s12517-021-06859-0>
- Hamzeh NH, Kaskaoutis DG, Rashki A, Mohammadpour K (2021b) Long-term variability of dust events in Southwestern Iran and its relationship with the drought. *Atmos*. <https://doi.org/10.3390/atmos12101350>
- Hoffmann C, Funk R, Wieland R, Li Y, Sommer M (2008) Effects of grazing and topography on dust flux and deposition in the Xilinge grassland, Inner Mongolia. *J Arid Environ* 72:792–807. <https://doi.org/10.1016/j.jaridenv.2007.09.004>
- Holloway J, Mengersen K (2018) Statistical machine learning methods and remote sensing for sustainable development goals: a review. *Remote Sens* 10. <https://doi.org/10.3390/rs10091365>
- Hossein Hamzeh N, Karami S, Kaskaoutis D, Tegen I, Moradi M, Opp C (2021) Atmospheric dynamics and numerical simulations of six frontal dust storms in the Middle East region. *Atmosphere (Basel)* 12:125. <https://doi.org/10.3390/atmos12010125>
- Hu Z, Kang S, Li X, Li C, Sillanpää M (2020) Relative contribution of mineral dust versus black carbon to Third Pole glacier melting. *Atmos Environ* 223:117288. <https://doi.org/10.1016/j.atmosenv.2020.117288>
- Jiao P, Wang J, Chen X, Ruan J, Ye X, Alavi AH (2021) Next-generation remote sensing and prediction of sand and dust storms: State-of-the-art and future trends. *Int J Remote Sens* 42:5277–5316. <https://doi.org/10.1080/01431161.2021.1912433>
- Kang L, Huang J, Chen S, Wang X (2016) Long-term trends of dust events over Tibetan Plateau during 1961–2010. *Atmos Environ* 125:188–198. <https://doi.org/10.1016/j.atmosenv.2015.10.085>
- Karami S, Kaskaoutis DG, Kashani SS, Rahnama M, Rashki A (2021) Evaluation of nine operational models in forecasting different types of synoptic dust events in the Middle East. *Geosci*. <https://doi.org/10.3390/geosciences11110458>
- Kendall MA (1949) Rank Correlation Methods. By Maurice G. Kendall, M.A. [Pp. vii + 160. London: Charles Griffin and Co. Ltd., 42 Drury Lane, 1948. 18s.]. *J Inst Actuar* 75:140–141. <https://doi.org/10.1017/S0020268100013019>
- Khaniabadi YO, Daryanoosh SM, Amrane A, Polosa R, Hopke PK, Goudarzi G, Mohammadi MJ, Sicard P, Armin H (2017) Impact of Middle Eastern dust storms on human health. *Atmos Pollut Res* 8:606–613. <https://doi.org/10.1016/j.apr.2016.11.005>
- Khoshakhlagh F, Najafi MS, Samadi M (2012) An analysis on synoptic patterns of springtime dust occurrence in West of Iran. *Phys*

- Geogr Res Q 44:99–124. <https://doi.org/10.22059/jphgr.2012.29209>
- Kim H, Choi M (2015) Impact of soil moisture on dust outbreaks in East Asia: using satellite and assimilation data. *Geophys Res Lett* 42:2789–2796. <https://doi.org/10.1002/2015GL063325>
- Lary DJ, Alavi AH, Gandomi AH, Walker AL (2016) Machine learning in geosciences and remote sensing. *Geosci Front* 7:3–10. <https://doi.org/10.1016/j.gsf.2015.07.003>
- Ledari DG, Hamidi M, Shao Y (2022) Numerical simulation of the 18 February 2017 frontal dust storm over southwest of Iran using WRF-Chem, satellite imagery, and PM10 concentrations. *J Arid Environ* 196:104637. <https://doi.org/10.1016/j.jaridenv.2021.104637>
- Liakos KG, Busato P, Moshou D, Pearson S, Bochtis D (2018) Machine learning in agriculture: a review. *Sensors* 18. <https://doi.org/10.3390/s18082674>
- Mahendra HN, Mallikarjunaswamy S, Kumar DM, Kumari S, Kashyap S, Fulwani S, Chatterjee A (2023) Assessment and prediction of air quality level using ARIMA model: a case study of Surat City, Gujarat State, India. *Nat Environ and Pollut Technol* 22:199–210
- Mahmoodirad A, Dehghan R, Niroomand S (2019) Modelling linear fractional transportation problem in belief degree—based uncertain environment. *J Exp Theor Artif Intell* 31:393–408. <https://doi.org/10.1080/0952813X.2018.1552318>
- Mahmoodirad A, Sanei M (2015) Solving a multi-stage multi-product solid supply chain network design problem by meta-heuristics. *Sci Iran* 23. <https://doi.org/10.24200/sci.2016.3908>
- Mann HB (1945) Nonparametric tests against trend. *Econometrica* 13:245–259. <https://doi.org/10.2307/1907187>
- Mashat A-WS, Awad AM, Assiri ME, Labban AH (2020) Dynamic and synoptic study of spring dust storms over northern Saudi Arabia. *Theor Appl Climatol* 140:619–634. <https://doi.org/10.1007/s00704-020-03095-6>
- Mehrzi E (2020) An investigation of sources of dust storms in the southeast and southwest regions of Iran to cite this version : HAL Id : hal-02586232. First Int. Conf. Dust Storms.
- Middleton N, Kashani SS, Attarchi S, Rahnama M, Mosalman ST (2021) Synoptic causes and socio-economic consequences of a severe dust storm in the Middle East. *Atmosphere (Basel)* 12. <https://doi.org/10.3390/atmos12111435>
- Middleton N, Tozer P, Tozer B (2019) Sand and dust storms: underrated natural hazards. *Disasters* 43:390–409. <https://doi.org/10.1111/disa.12320>
- Middleton NJ (2017) Desert dust hazards: a global review. *Aeolian Res* 24:53–63. <https://doi.org/10.1016/j.aeolia.2016.12.001>
- Modarres R (2021) Dust storm frequency change in relation to climate drivers. *Int J Climatol* 41:E187–E199. <https://doi.org/10.1002/joc.6675>
- Mohammadpour K, Siortino M, Saligheh M, Raziie T, Darvishi Boloorani A (2020) Spatiotemporal regionalization of atmospheric dust based on multivariate analysis of MACC model over Iran. *Atmos Res*. <https://doi.org/10.1016/j.atmosres.2020.105322>
- Molla-Alizadeh-Zavardehi S, Mahmoodirad A, Rahimian M (2014) Step fixed charge transportation problems via genetic algorithm. *Indian J Sci Technol* 7:949–954. <https://doi.org/10.17485/ijst/2014/v7i7.5>
- Munkhtsetseg E, Shinoda M, Gillies JA, Kimura R, King J, Nikolich G (2016) Relationships between soil moisture and dust emissions in a bare sandy soil of Mongolia. *Particuology* 28:131–137. <https://doi.org/10.1016/j.partic.2016.03.001>
- Nabavi SO, Haimberger L, Abbasi R, Samimi C (2018) Prediction of aerosol optical depth in West Asia using deterministic models and machine learning algorithms. *Aeolian Res* 35:69–84. <https://doi.org/10.1016/j.aeolia.2018.10.002>
- Nafarzadegan AR, Ebrahimi-Khusfi Z, Kazemi M (2021) Spatial characterization of dust emission prone arid regions using feature extraction and predictive algorithms. *Appl Geogr* 133:102495. <https://doi.org/10.1016/j.apgeog.2021.102495>
- Namdari S, Karimi N, Sorooshian A, Mohammadi G, Sehatkashani S (2018) Impacts of climate and synoptic fluctuations on dust storm activity over the Middle East. *Atmos Environ* 173:265–276. <https://doi.org/10.1016/j.atmosenv.2017.11.016>
- Niroomand S, Garg H, Mahmoodirad A (2020) An intuitionistic fuzzy two stage supply chain network design problem with multi-mode demand and multi-mode transportation. *ISA Trans* 107:117–133. <https://doi.org/10.1016/j.isatra.2020.07.033>
- Orlovsky N, Orlovsky L, Indoitu R (2013) Severe dust storms in Central Asia. *Arid Ecosyst* 3. <https://doi.org/10.1134/S2079096113040082>
- Papadopoulou K, Alasis C, Xydis G (2019) On the wind blade’s surface roughness due to dust accumulation and its impact on the wind turbine’s performance: a heuristic QBlade-based modelling assessment. *Environ Prog Sustain Energy* 39:e13296. <https://doi.org/10.1002/ep.13296>
- Papi R, Kakroodi AA, Soleimani M, Karami L, Amiri F, Alavipanah SK (2022) Identifying sand and dust storm sources using spatial-temporal analysis of remote sensing data in Central Iran. *Ecol Inform* 70:101724. <https://doi.org/10.1016/j.ecoinf.2022.101724>
- Rayegani B, Barati S, Goshtasb H, Gachpaz S, Ramezani J, Sarkheil H (2020) Sand and dust storm sources identification: a remote sensing approach. *Ecol Indic* 112:106099. <https://doi.org/10.1016/j.ecolind.2020.106099>
- Rezazadeh M, Irannejad P, Shao Y (2013) Climatology of the Middle East dust events. *Aeolian Res* 10:103–109. <https://doi.org/10.1016/j.aeolia.2013.04.001>
- Silva Junior CHL, Almeida CT, Santos JRN, Anderson LO, Aragão LEOC, Silva FB (2018) Spatiotemporal rainfall trends in the Brazilian Legal Amazon between the years 1998 and 2015. *Water*. <https://doi.org/10.3390/w10091220>
- Shafiee M, Behnamian H, Feghhi, SAH (2017) A study of wake potentials for the pick-ups in storage ring. *J Instrum* 12:T12006–T12006. <https://doi.org/10.1088/1748-0221/12/12/T12006>
- Shafiee M, Grossan B, Hu J, Colantoni I, Smoot G (2019) Design optimization of a 10 kilopixel optical band Microwave Kinetic Inductance Detector. *J Instrum* 14:P12011–P12011. <https://doi.org/10.1088/1748-0221/14/12/p12011>
- Soleimani Z, Teymouri P, Darvishi Boloorani A, Mesdaghinia A, Middleton N, Griffin DW (2020) An overview of bioaerosol load and health impacts associated with dust storms: A focus on the Middle East. *Atmos Environ* 223:117187. <https://doi.org/10.1016/j.atmosenv.2019.117187>
- Vishkaee F, Flamant C, Cuesta J, Flamant P, Khalesifard H (2011) Multiplatform observations of dust vertical distribution during transport over Northwest Iran in the Summertime. *J Geophys Res Atmos* 116. <https://doi.org/10.1029/2010JD014573>
- Wilkerson WD (1991) Dust and sand forecasting in Iraq and adjoining countries
- Yin Z, Wan Y, Zhang Y, Wang H (2021) Why super sandstorm 2021 in North China. *Natl Sci Rev* 9. <https://doi.org/10.1093/nsr/nwab165>

**Publisher’s note** Springer Nature remains neutral with regard to jurisdictional claims in published maps and institutional affiliations.

Springer Nature or its licensor (e.g. a society or other partner) holds exclusive rights to this article under a publishing agreement with the author(s) or other rightsholder(s); author self-archiving of the accepted manuscript version of this article is solely governed by the terms of such publishing agreement and applicable law.

## Authors and Affiliations

Parya Broomandi<sup>1,2</sup> · David Galán-Madruga<sup>3</sup> · Alfredo Satyanaga<sup>1</sup> · Mehdi Hamidi<sup>4</sup> · Dorna Gholamzade Ledari<sup>5</sup> · Aram Fathian<sup>6,7,8</sup> · Rasoul Sarvestan<sup>9</sup> · Nasime Janatian<sup>10,11</sup> · Ali Jahanbakhshi<sup>12</sup> · Mehdi Bagheri<sup>2</sup> · Ferhat Karaca<sup>1,13</sup> · Ali Al-Dousari<sup>14</sup> · Jong Ryeol Kim<sup>1</sup>

<sup>1</sup> Department of Civil and Environmental Engineering, School of Engineering and Digital Sciences, Nazarbayev University, Kabanbay Batyr Ave. 53, Nur-Sultan, Kazakhstan 010000

<sup>2</sup> Department of Electrical and Computer Engineering, School of Engineering and Digital Sciences, Nazarbayev University, Kabanbay Batyr Ave. 53, Nur-Sultan, Kazakhstan 010000

<sup>3</sup> Department of Atmospheric Pollution, National Centre for Environment Health, Health Institute Carlos III, Ctra. Majadahonda a Pozuelo km 2.2, 28220 Madrid, Spain

<sup>4</sup> Faculty of Civil Engineering, Babol Noshirvani University of Technology, Babol, Iran

<sup>5</sup> School of Civil Engineering, University of Tehran, Tehran, Iran

<sup>6</sup> Neotectonics and Natural Hazards Institute, RWTH Aachen University, Aachen, Germany

<sup>7</sup> UNESCO Chair on Coastal Geo-Hazard Analysis, Research Institute for Earth Sciences, Tehran, Iran

<sup>8</sup> Water, Sediment, Hazards, and Earth-surface Dynamics (waterSHED) Lab, Department of Geoscience, University of Calgary, Calgary, Canada

<sup>9</sup> Department of Climatology, Faculty of Geography and Environmental Sciences, Hakim Sabzevari University, Sabzevar, Iran

<sup>10</sup> Department of Geoscience and Engineering, Faculty of Civil Engineering and Geosciences, Delft University of Technology, Stevinweg 1, 2628 Delft, CN, Netherlands

<sup>11</sup> Department of Marine Systems, Division of Modelling and Remote Sensing, Tallinn University of Technology (Taltech), Tallinn, Estonia

<sup>12</sup> School of Architecture, Building and Civil Engineering, Loughborough University, Loughborough, UK

<sup>13</sup> Environment and Resource Efficiency Cluster (EREC), Nazarbayev University, Kabanbay Batyr Ave. 53, Nur-Sultan, Kazakhstan 010000

<sup>14</sup> Crisis Decision Support Program, Environment and Life Sciences Research Center, Kuwait Institute for Scientific Research, Kuwait City, Kuwait